

# On the Use of a Regular Yield Surface for the Analysis of Unreinforced Masonry Walls

[P.G. Asteris](#) and [A.D. Tzamtzis](#)

Department of Civil Works Technology Technological Educational Institution of Athens, Greece.

Email: [asteris@teiath.gr](mailto:asteris@teiath.gr)

---

## ABSTRACT

A complete methodology for the non-linear macroscopic analysis of unreinforced masonry (URM) shear walls under biaxial stress state is presented, using the finite element method. The methodology focuses on the definition / specification of a general anisotropic (orthotropic) failure surface of masonry under biaxial stress, using a cubic tensor polynomial, as well as on the numerical solution of this non-linear problem. The characteristics of the polynomial used, ensure the closed shape of the failure surface which is expressed in a unique mathematical form for all possible combinations of plane stress, making it easier to include it into existing software for the analysis of masonry structures. The validity of the method, using the derived failure surface, is demonstrated by comparing the results from the study of the non-linear behaviour of URM wall panels, under uniform compressive and shear loading, against results derived by other investigators.

## KEYWORDS

Anisotropic behaviour, masonry, non-linear analysis, shear wall, yield pattern, yield surface.

---

## 1 Introduction

Analytical and experimental studies on the behaviour of masonry walls to in-plane static loads have been the focus of activity of a number of investigators for many years. Masonry exhibits distinct directional properties, due to the influence of mortar joints acting as planes of weakness. Depending upon the orientation of the joints to the stress directions, failure can occur in the joints alone, or simultaneously in the joints and blocks. The great number of the influencing factors, such as dimension and anisotropy of the bricks, joint width and arrangement of bed and head joints, material properties of both brick and mortar, and quality of workmanship, make the simulation of plain brick masonry extremely difficult.

The failure of masonry under uniaxial and biaxial stress states has been studied extensively in the past. These failures all represent particular points on the general failure surface. The development of a general yield criterion for masonry is difficult, because of the difficulties in developing a representative biaxial test and the large number of tests involved.

In the absence of a suitable model to represent its behaviour, in the past masonry was assumed to be an isotropic elastic continuum; consequently, the influence of the mortar joints acting as planes of weakness, could not be addressed. The development of improved models of material behaviour was made possible by the increased sophistication of numerical methods of stress analysis. Indeed, it is only recently that analytical procedures, which account for the non-linear behaviour of masonry under static loads, have been developed. These analytical procedures could be summarized in the following two levels of refinement for masonry models:

- **Macro-modelling (masonry as an one-phase material):** According to this procedure [1, 2], no distinction between the individual units and joints is made, and masonry is considered as a homogeneous, isotropic or anisotropic continuum. While this procedure may be preferred for the analysis of large masonry structures, it is not suitable for the detailed stress analysis of a small panel, due to the fact that it is difficult to capture all its

failure mechanisms. The influence of the mortar joints acting as planes of weakness cannot be addressed.

- **Micro-modelling (masonry as a multi-phase material):** According to this procedure [3, 4, 5, 6, 7], the units, the mortar, and the unit/mortar interface, are modeled separately. While this leads to more accurate results, the level of refinement means that any analysis will be computationally intensive, and so will limit its application to small laboratory specimens and structural details. A.D. Tzamtzis [8] and Sutcliffe et al. [9], have recently proposed simplified micro-modelling procedures to overcome the problem. According to these procedures, which are intermediate approaches, the properties of the mortar and the unit/mortar interface (masonry as a two-phase material) are lumped into a common element, while expanded elements are used to represent the brick units. This approach leads to the reduction in computational intensiveness, and yields a model, which is applicable to a wider range of structures.

In the present work, a complete methodology for the non-linear analysis of anisotropic masonry shear walls under biaxial stress state is presented, regarding masonry as an one-phase material. One of the advantages of the proposed material model is that average properties, which include the influence of both brick and joint, have been used. This means that a relatively coarse finite element mesh can be used with any element typically encompassing several bricks and joints. This has considerable computational advantages when analysing large wall panels.

The basic assumptions and the associated mathematical expressions of the theory of plasticity are first outlined, giving special attention to their formulation for the case of anisotropic masonry. The significance of the use of a regular yield surface for the description of yield has been manifested since 1950, and introduced by Hill in his book “The Mathematical Theory of Plasticity” [10]. It is to be noted that the use of a failure surface that consists of more than one type of surface could demand additional effort in the analysis process of the masonry structure. According to Zienkiewicz et al. [11], the computation of singular points (“corners”) on failure surfaces may be avoided by a suitable choice of a continuous surface, which can usually represent the true condition.

The main aim of this paper is the introduction of a regular yield surface; that is, a surface defined by a single equation of the form  $f(\sigma)=0$  [12], to define failure under biaxial stress for masonry. This has been accomplished using a cubic tensor polynomial the characteristics of which ensures the closed shape of the failure surface and can represent, with a good degree of accuracy, the real masonry behaviour (experimental data) under failure conditions. It is to be shown that the geometry of the yield surface tends to have a significant influence not only in the formulation, but also in the numerical solution of the non-linear problem.

An additional problem in present-day-practice is that the non-linear analysis of the behaviour of masonry is usually performed with the use of ready-made software packages that have been developed mainly for the analysis of concrete structures [13, 14]. The main disadvantage in using these ready-made programs is that their architecture is not amenable to modifications and, therefore, they cannot take into account important features appropriate for the case of masonry.

To overcome this problem, a novel computer code, in FORTRAN programming language, has been developed for the structural design and analysis of URM shear walls. The code can be applied for the analysis of elasto-plastic anisotropic URM walls under plane stress. During the development procedure, special attention has been given at the graphic imaging of the analysis results. The program possesses the capability of automatic mesh generation, and produces the load – displacement diagram, giving a coloured graphic image of the yield pattern within the structure, for every increment of load.

## 2 Basic mathematical aspects of the non-linear analysis

In order to formulate a theoretical description capable to model elasto-plastic material deformation, three requirements have to be met:

- An explicit relationship between stress and strain that will describe the material's behavior under elastic conditions must be expressed
- A yield criterion that will define the stress level at which plastic flow commences must be postulated, and
- A relationship between stress and strain must be developed for post-yield behavior; i.e., when the deformation is made up of both elastic and plastic components.

The relationship between stress and strain, before the onset of plastic yielding, is given by the following standard linear elastic expression:

$$\sigma = D\varepsilon \quad (1)$$

In this expression  $\sigma$  and  $\varepsilon$  are the stress and strain components, respectively, and  $D$  is the elasticity matrix.

Masonry walls exhibit distinct directional properties due to the influence of mortar joints acting as planes of weakness. In particular, the material of masonry shows a different modulus of elasticity ( $E_x$ ) in the  $x$  direction (direction parallel to the bed joints of masonry) and a different modulus of elasticity ( $E_y$ ) in the  $y$  direction (perpendicular to the bed joints). In the case of plane stress, the elasticity matrix is defined by

$$D = \begin{bmatrix} \frac{E_x}{1-\nu_{xy}\nu_{yx}} & \frac{E_x\nu_{yx}}{1-\nu_{xy}\nu_{yx}} & 0 \\ \frac{E_y\nu_{xy}}{1-\nu_{xy}\nu_{yx}} & \frac{E_y}{1-\nu_{xy}\nu_{yx}} & 0 \\ 0 & 0 & G_{xy} \end{bmatrix} \quad (2)$$

in which  $\nu_{xy}$ ,  $\nu_{yx}$  are the Poisson's ratios in the  $xy$  and  $yx$  plane respectively; and  $G_{xy}$  is the shear modulus in the  $xy$  plane. It is worth noticing that in the case of plane stress in an anisotropic material the following equation holds

$$E_x\nu_{yx} = E_y\nu_{xy} \quad (3)$$

In this work, masonry is assumed to be a homogeneous and anisotropic material.

### 2.1 The yield criterion

The yield criterion defines the stress level at which plastic deformation begins and takes the form of the equation:

$$f(\sigma) = 0 \quad (4)$$

where  $f$  is a function.

### 2.2 Plastic flow rule

Von Mises first suggested the basic constitutive relation that defines the plastic strain increments in relation to the yield surface. Various other researchers [15, 16] have proposed

heuristic methods for the validation of Von Mises relationship. These methods have led to the current state-of-the-art hypothesis, which states that:

If  $\delta\{\varepsilon\}_p$  denotes the increment of plastic strain, then:

$$\delta\{\varepsilon\}_p = \lambda \frac{\partial f}{\partial \{\sigma\}} \quad (5)$$

where  $\lambda$  is a determinable constant (plastic multiplier).

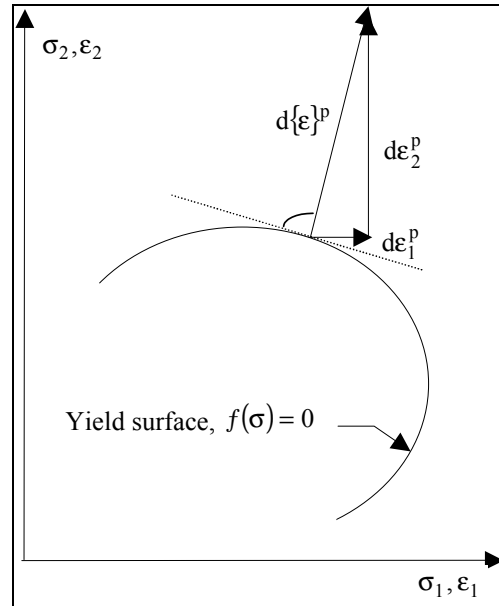


**Figure 1:** Geometrical representation of the normality rule in 2D Stress Space.

This rule is widely known as the normality principle because the relation (5) can be interpreted as requiring the normality of the plastic strain increment vector to the yield surface in the hyper-space of  $v$  stress dimensions. In [Figure 1](#), this normality rule is shown, in the case of a two dimensional space.

### 2.3 Stress-strain relations

During an infinitesimal increment of stress, changes of strain are assumed to be partly elastic and partly plastic as

$$\delta\{\varepsilon\} = \delta\{\varepsilon\}_e + \delta\{\varepsilon\}_p \quad (6)$$

The elastic strain increments are related to the stress increments via a symmetric matrix of constants  $[D]$  known as the elasticity matrix:

$$\delta\{\varepsilon\}_e = [D]^{-1} \delta\{\sigma\} \quad (7)$$

Expression (6) can be readily rewritten as

$$\delta\{\varepsilon\} = [D]^{-1} \delta\{\sigma\} + \frac{\partial f}{\partial \{\sigma\}} \lambda \quad (8)$$

When plastic yield is occurring the stresses are on the yield surface given by (4). By differentiating this we have

$$0 = \frac{\partial f}{\partial \sigma_x} \delta\sigma_x + \frac{\partial f}{\partial \sigma_y} \delta\sigma_y + \dots$$

or

$$0 = \left\{ \frac{\partial f}{\partial \{\sigma\}} \right\}^T \delta\{\sigma\} \quad (9)$$

or

$$0 = \alpha^T \delta\{\sigma\} \quad (10)$$

where:

$$\alpha = \left\{ \frac{\partial f}{\partial \{\sigma\}} \right\} \quad (11)$$

The vector  $\alpha$  is termed flow vector. It should be mentioned that vector  $\delta\{\sigma\}$  of the stress increment is perpendicular to the flow vector  $\alpha$  since their inner product equals zero (10). Equation (8) can therefore take the following form:

$$\delta\{\varepsilon\} = [D]^{-1} \delta\{\sigma\} + \alpha\lambda \quad (12)$$

Left-handed multiplying both sides of equation (12) by  $\alpha^T D$  we obtain:

$$\alpha^T D \delta\{\varepsilon\} = \alpha^T \delta\{\sigma\} + \alpha^T D \alpha \lambda \quad (13)$$

The first term of the right-hand of Eq. (13) is zero, according to Eq. (10). Therefore, Eq. (13) becomes:

$$\alpha^T D \delta\{\varepsilon\} = \alpha^T D \alpha \lambda$$

Solving for plastic multiplier  $\lambda$ , we obtain:

$$\lambda = \frac{\alpha^T D \delta\{\varepsilon\}}{\alpha^T D \alpha} \quad (14)$$

Substituting Eq. (14) into Eq. (12), we obtain:

$$\delta\{\varepsilon\} = D^{-1} \delta\{\sigma\} + \alpha \frac{\alpha^T D \delta\{\varepsilon\}}{\alpha^T D \alpha}$$

Solving for  $\delta\{\sigma\}$ , we obtain:

$$\delta\{\sigma\} = D \left[ 1 - \frac{\alpha \alpha^T D}{\alpha^T D \alpha} \right] \delta\{\varepsilon\}$$

or

$$\delta\{\sigma\} = D_{ep} \delta\{\varepsilon\} \quad (15)$$

where:

$$D_{ep} = D - \frac{D \alpha \alpha^T D}{\alpha^T D \alpha} \quad (16)$$

is the elasto-plastic matrix.

### 3 The method of initial stress for the solution of the elasto-plastic problem

Zienkiewicz, Valliapan and King [11] proposed in 1969 the method of initial stress that can solve an elasto-plastic problem based on a series of successive approximations. In the first step of the computation, during a load increment, a purely elastic problem is solved determining an

increment of strain  $\Delta\epsilon'$  and the relevant increment of stress  $\Delta\sigma'$  at every point of construction. The non-linearity of the problem implies however that for the increment of strain found, the stress increment will in general not be correct. If  $\Delta\sigma$  is the real increment of stress for the given strain, then the situation can only be maintained by a set of body forces equilibrating the initial stress system  $(\Delta\sigma - \Delta\sigma')$ .

At the second step of the computation we can remove all previous body forces by allowing the structure (with unchanged elastic properties) to have a new deformation. This way, additional new strain, and the corresponding stress increments, will be caused. However, these are most likely to exceed those permissible by the non-linear relationship and redistribution of the equilibrating body forces has to be repeated.

If the process converges within a load increment, the full non-linear compatibility and equilibrium conditions will be satisfied, just as they are in an incremental elasticity solution. As all applications show, this convergence is very fast and three or four cycles of redistribution (iterations) are sufficient in any load increment.

In order to follow the flow rules of plasticity, we must apply a series of load increments. If, however, a single load increment is used, it will be found that an approximate lower bound is achieved, satisfying equilibrium and yield criteria but not necessarily following the current strain development.

For the elasto-plastic case the steps during a typical load increment can be summarized as follows:

- Step 1.** Apply load increment and determine elastic increments of stress  $\{\Delta\sigma'\}_1$  and strain  $\{\Delta\epsilon'\}_1$  which correspond.
- Step 2.** Add  $\{\Delta\sigma'\}_1$  to stresses existing at start of increment  $\{\sigma_0\}$  to obtain  $\{\sigma'\}$ . Check whether  $f\{\sigma'\} < 0$ . If above satisfied, only elastic strain changes occur and the process is stopped, if not proceed to 3.
- Step 3.** If  $f\{\sigma'\} \geq 0$  and also  $f\{\sigma_0\} = 0$  (i.e. element was in yield at start of increment), compute  $\{\Delta\sigma\}_1$  by equation (15).

$$\{\Delta\sigma\}_1 = [D]_{ep} \{\Delta\epsilon'\}_1$$

where  $[D]_{ep}$  is computed from equation (16) using stresses  $\{\sigma'\}$ .

Evaluate stress which has to be supported by body forces

$$\{\Delta\sigma''\}_1 = \{\Delta\sigma'\}_1 - \{\Delta\sigma\}_1$$

Store current stress  $\{\sigma\} = \{\sigma'\} - \{\Delta\sigma''\}_1$

And current strain  $\{\epsilon\} = \{\epsilon'\} + \{\Delta\epsilon'\}_1$

- Step 4.** If  $f\{\sigma'\} \geq 0$  and  $f\{\sigma_0\} < 0$  find the intermediate stress value at which yield begins and compute increment  $\{\Delta\sigma\}_1$  by equation (15) starting from that point. Then proceed as in third step.

- Step 5.** Compute nodal forces corresponding to the equilibrating body forces. These are given for any finite element by

$$\{P\} = \int [B]^T \{\Delta\sigma'\}_1 d(\text{vol})$$

**Step 6.** Resolve using original elastic properties and the load system  $\{P\}$  to find  $\{\Delta\sigma'\}_2$  and  $\{\Delta\varepsilon'\}_2$ .

**Step 7.** Repeat steps 2 to 6.

The cycling is terminated when the nodal forces of fifth step reach sufficiently small values. If this is not achieved in a predetermined number of cycles (20 in our case) collapse condition is deemed to have been achieved and the process is stopped. The computational procedure is illustrated graphically in a two-dimensional stress space in [Figure 2](#).

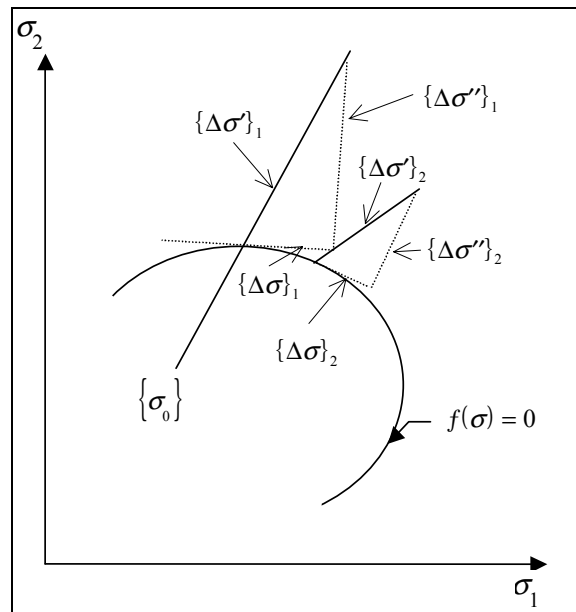


**Figure 2:** Graphical Interpretation of the Initial Stress Method.

## 4 Yield surface geometry effect in non-linear solution

In this paragraph a description is made on the effect the yield surface geometry has in the formulation and the numerical solution of the elasto-plastic problem.

### 4.1 “Corners” in a yield surface

Sometimes the yield surface is not defined by only a single continuous (and convex) function, but by a series of functions:

$$f_1, f_2, \dots, f_n$$

According to Koiter [12], a surface of this kind is called singular. Such a surface is the yield surface of Tresca and the yield surface for masonry, in three mutually intersected cones, proposed by Dhanasekar, Page, and Kleeman [22].

For most of the bounding surface, only a single condition such as  $f_m = 0$  can define the yield surface, and the previously written flow rules apply.

At a singular point (“corner”) of the yield surface we may have, however, the condition that

$$f_h = \dots = f_m = 0$$

For such a singular point, the use of the following equation has been proposed by Koiter [12], for the estimation of the increment of plastic strain, instead of equation 5:

$$d\{\varepsilon_p\} = \lambda_h \left\{ \frac{\partial f_h}{\partial \{\sigma_h\}} \right\} + \dots + \lambda_m \left\{ \frac{\partial f_m}{\partial \{\sigma_m\}} \right\} \quad (17)$$

where  $\lambda_i$  are positive constants (Figure 3).

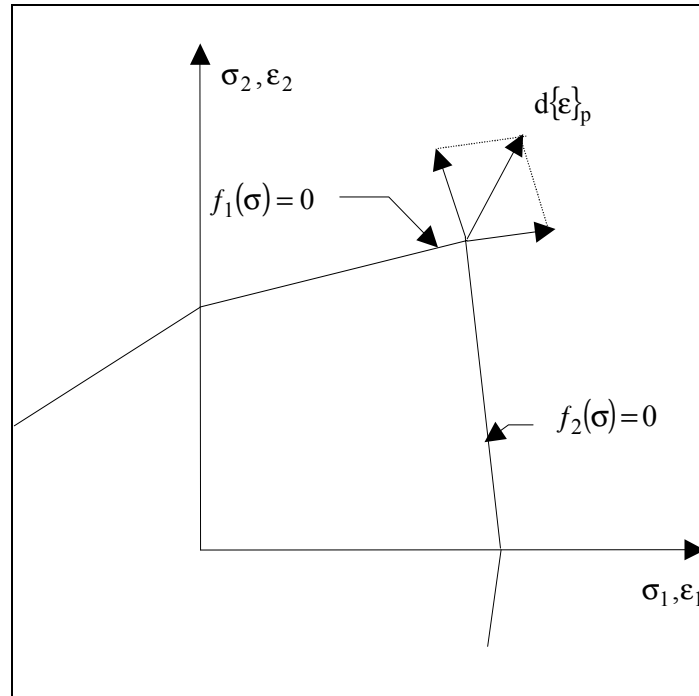


Figure 3 Corners in a yield surface. Graphical interpretation of Koiter's criterion.

According to Zienkiewicz, Valliapan, and King [11], the use of singular areas imposes important problems to the elasto-plastic analysis process. The authors propose to avoid calculating the singular points in a yield surface, by making a suitable choice of continuous surfaces, which can usually represent the true condition with a good degree of accuracy.

#### 4.2 Development of a realistic failure criterion for masonry under biaxial stress

The failure theories for isotropic materials are not applicable for masonry under biaxial stresses because they are derived on the basis of the invariant state of stress concept where the stress orientation has no effect on the strength. In this section, failure criteria are proposed as a generalized form for masonry under biaxial stresses, taking into consideration its anisotropic nature as a composite material. The mortar bed joints, because of their continuous nature, divide the media into layers of equal thickness and thus give masonry the appearance of a laminated composite material. For the expression of an analytical failure model of masonry, therefore, a polynomial that is available already for composite materials is proposed. This failure surface in the stress space, can be described by the equation [17, 18, 19]:

$$f(\sigma_\ell) = F_i \sigma_i + F_{ij} \sigma_i \sigma_j + F_{ijk} \sigma_i \sigma_j \sigma_k + \dots - 1 = 0 \quad (18)$$

In this equation  $\sigma_\ell$  ( $\ell = 1, 2, \dots, 6$ ) are the components of stresses and  $F_i, F_{ij}, F_{ijk}$  ( $i, j, k = 1, 2, \dots, 6$ ) are coefficients to be properly determined.

If one restricts the analysis to a plane stress state and considers that a cubic formulation is reasonably accurate representation of the failure surface, then Equation (18) reduces to:

$$\begin{aligned}
 &F_1\sigma_1 + F_2\sigma_2 + F_6\sigma_6 + F_{11}\sigma_1^2 + F_{12}\sigma_1\sigma_2 + F_{16}\sigma_1\sigma_6 + F_{21}\sigma_2\sigma_1 + F_{22}\sigma_2^2 + F_{26}\sigma_2\sigma_6 + \\
 &+ F_{61}\sigma_6\sigma_1 + F_{62}\sigma_6\sigma_2 + F_{66}\sigma_6^2 + F_{111}\sigma_1^3 + F_{112}\sigma_1^2\sigma_2 + F_{116}\sigma_1^2\sigma_6 + F_{121}\sigma_1^2\sigma_2 + \\
 &+ F_{122}\sigma_1\sigma_2^2 + F_{126}\sigma_1\sigma_2\sigma_6 + F_{161}\sigma_1^2\sigma_6 + F_{162}\sigma_1\sigma_2\sigma_6 + F_{166}\sigma_1\sigma_6^2 + F_{211}\sigma_2\sigma_1^2 + \\
 &+ F_{212}\sigma_1\sigma_2^2 + F_{216}\sigma_1\sigma_2\sigma_6 + F_{221}\sigma_1\sigma_2^2 + F_{222}\sigma_2^3 + F_{226}\sigma_2^2\sigma_6 + F_{261}\sigma_1\sigma_2\sigma_6 + \\
 &+ F_{262}\sigma_2^2\sigma_6 + F_{266}\sigma_2\sigma_6^2 + F_{611}\sigma_1^2\sigma_6 + F_{612}\sigma_1\sigma_2\sigma_6 + F_{616}\sigma_1\sigma_6^2 + F_{621}\sigma_1\sigma_2\sigma_6 + \\
 &+ F_{622}\sigma_2^2\sigma_6 + F_{626}\sigma_2\sigma_6^2 + F_{661}\sigma_1\sigma_6^2 + F_{662}\sigma_2\sigma_6^2 + F_{666}\sigma_6^3 - 1 = 0
 \end{aligned}$$

(19)

The following assumptions have been made [20, 21]:

- Symmetry of the material is assumed by the identity of “symmetric” coefficients, for  $i \neq j \neq k \neq i$ , that is  $F_{ijk} = F_{ikj} = F_{jik} = F_{kij} = F_{kji} = F_{jki}$ , and  $F_{ij} = F_{ji}$ .
- The material under a given shear loading, possesses a common shear strength ( $S=S'$ ), for both positive or negative direction of shear loading. Consequently, assuming that there is no dependence on the shear loading direction, the terms with odd exponents of  $\sigma_6$ , can be eliminated.
- The redundant terms  $F_{iii}$  (for  $i = 1, 2$  and  $6$ ) are omitted.

Using the notations  $(\sigma_x, \sigma_y, \tau)$  instead of  $(\sigma_1, \sigma_2, \sigma_6)$ , equation 18 takes the form:

$$\begin{aligned}
 f(\sigma_x, \sigma_y, \tau) = &F_1\sigma_x + F_2\sigma_y + F_{11}\sigma_x^2 + F_{22}\sigma_y^2 + F_{66}\tau^2 + 2F_{12}\sigma_x\sigma_y + 3F_{112}\sigma_x^2\sigma_y + \\
 &3F_{122}\sigma_x\sigma_y^2 + 3F_{166}\sigma_x\tau^2 + 3F_{266}\sigma_y\tau^2 - 1 = 0
 \end{aligned}$$

(20)

Eliminating all third order terms in Eq. 20, a simplified yield criterion can be derived:

$$f(\sigma_x, \sigma_y, \tau) = F_1\sigma_x + F_2\sigma_y + F_{11}\sigma_x^2 + F_{22}\sigma_y^2 + F_{66}\tau^2 + 2F_{12}\sigma_x\sigma_y - 1 = 0 \quad (21)$$

This latter simple form of the yield criterion has already been used by other investigators [1, 22], to define the failure of brick masonry under biaxial stress state.

According to Symakezis and Asteris [21], the general yield criterion (Eq. 20) through its non-symmetric form, fit the non-symmetrically dispersed experimental data better than the simplified model (Eq. 21).

Using the above yield surfaces, the expression of flow vector is defined by

$$\alpha = \begin{Bmatrix} \frac{\partial f}{\partial \sigma_x} \\ \frac{\partial f}{\partial \sigma_y} \\ \frac{\partial f}{\partial \tau} \end{Bmatrix} = \begin{Bmatrix} F_1 + 2F_{11}\sigma_x + 2F_{12}\sigma_y + 6F_{112}\sigma_x\sigma_y + \\ \quad + 3F_{122}\sigma_y^2 + 3F_{166}\tau^2 \\ F_2 + 2F_{22}\sigma_y + 2F_{12}\sigma_x + 3F_{112}\sigma_x^2 + \\ \quad + 6F_{122}\sigma_x\sigma_y + 3F_{266}\tau^2 \\ 2F_{66}\tau + 6F_{166}\sigma_x\tau + 6F_{266}\sigma_y\tau \end{Bmatrix} \quad (22)$$

for the case of the general yield criterion, and by

$$\alpha = \begin{Bmatrix} \frac{\partial f}{\partial \sigma_x} \\ \frac{\partial f}{\partial \sigma_y} \\ \frac{\partial f}{\partial \tau} \end{Bmatrix} = \begin{Bmatrix} F_1 + 2F_{11}\sigma_x + 2F_{12}\sigma_y \\ F_2 + 2F_{22}\sigma_y + 2F_{12}\sigma_x \\ 2F_{66}\tau \end{Bmatrix} \quad (23)$$

for the case of the simplified yield criterion.

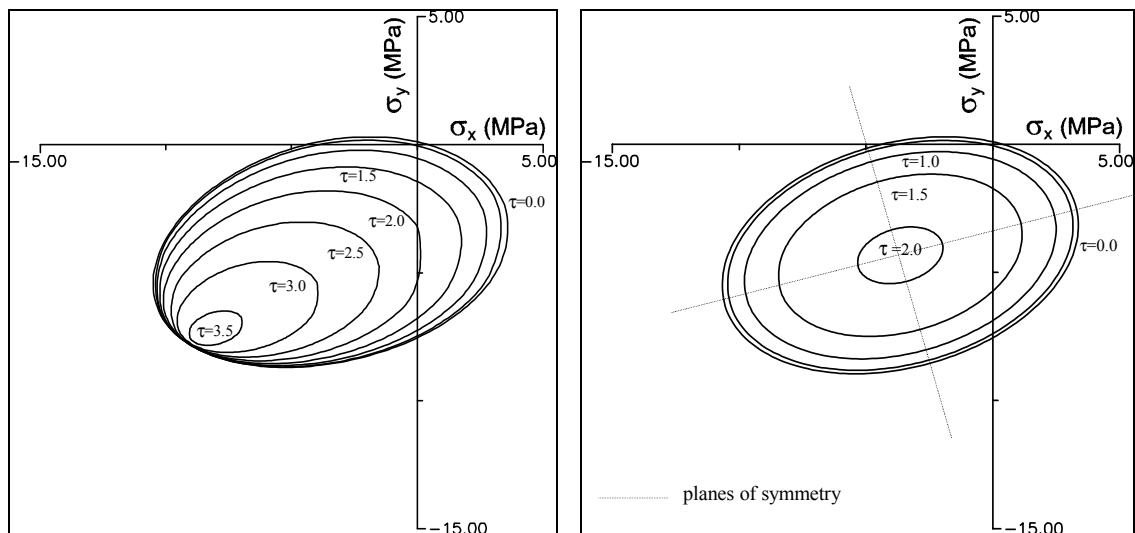
In order to determine the coefficients of the proposed polynomials (Eqs 20, 21), an evaluation of the mechanical characteristics of masonry is performed using the experimental data of Page [23], through a least squares approach. The regular yield surface (Figure 4a) for the case of the general yield criterion (Eq. 20), can then be defined as [2, 21]:

$$2.27\sigma_x + 9.87\sigma_y + 0.573\sigma_x^2 + 1.32\sigma_y^2 + 6.25\tau^2 - 0.30\sigma_x\sigma_y + 0.009585\sigma_x^2\sigma_y + 0.003135\sigma_x\sigma_y^2 + 0.28398\sigma_x\tau^2 + 0.4689\sigma_y\tau^2 = 1 \quad (24)$$

In addition, for the simplified yield criterion (Eq. 21), the regular yield surface (Figure 4b) can be defined as:

$$2.27\sigma_x + 9.87\sigma_y + 0.573\sigma_x^2 + 1.32\sigma_y^2 + 6.25\tau^2 - 0.454\sigma_x\sigma_y = 1 \quad (25)$$

The validity of the general yield criterion is demonstrated by comparing the derived analytical yield surface of Eq. 24 with the existing experimental results of Page [23]. More than 70 experimental data have been depicted in (Figure 5). In the same figure, analytical curves in principal stress terms are also depicted for the yield surface of eq. 24. The good agreement between the analytical and experimental data is apparent for this general yield surface with a non-symmetric curve.



(a) General yield criterion

(b) Simplified yield criterion

**Figure: 4** Yield surface of masonry in normal stress terms:

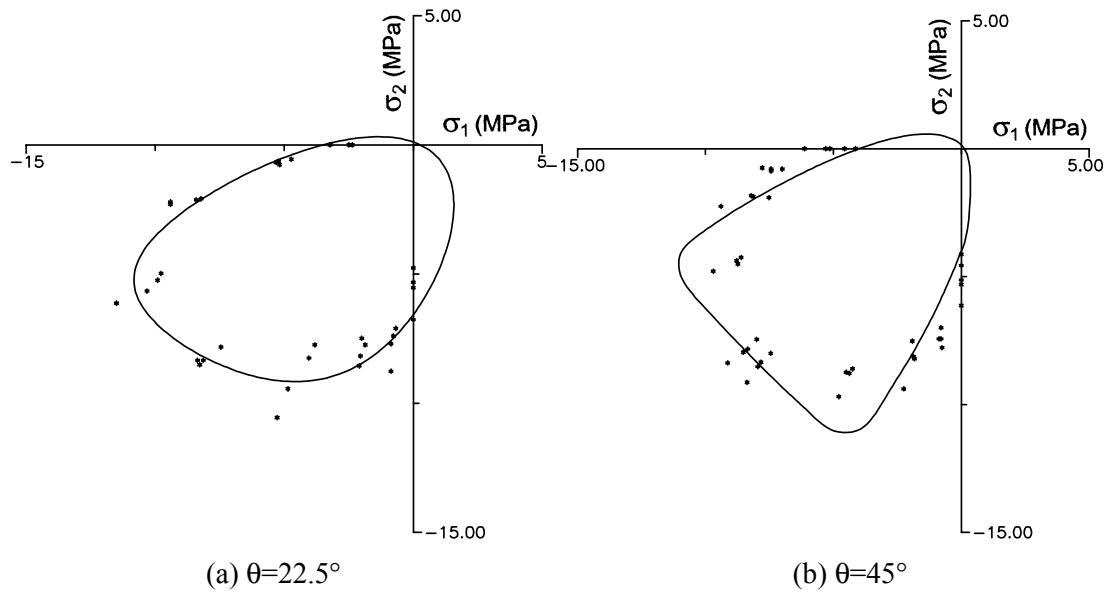


**Figure: 5** Yield curve of masonry in principal stress terms using the proposed general yield criterion

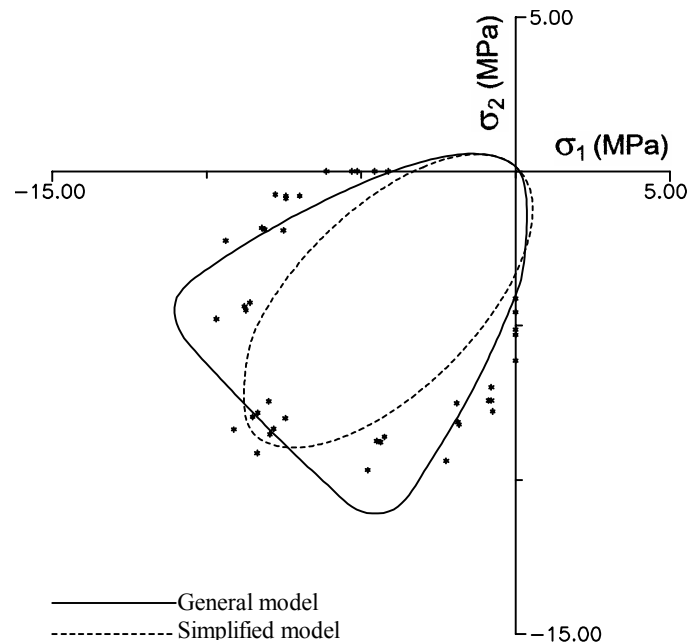


**Figure: 6** Yield curve of masonry in principal stress terms ( $\theta=45^\circ$ ).

In [Figure 6](#), the simplified model (dotted line) is compared with the general model (continuous line), for the case of an angle  $\theta$  (angle between the maximum principal stress direction and the direction of the x-axis) equal to  $45^\circ$ . It is to be noted that the general failure criterion through its non-elliptical (non-symmetric) form, can approach the non-elliptical dispersed experimental data of Page [\[23\]](#) better than the simplified model.

## 5 Computer code

In order to implement the proposed method of analysis, a specific finite element computer program for the 2D non-linear analysis of a masonry plane wall, under monotonic static loading,

has been developed. During the development procedure, we have made use of the ready-made databanks of Owen & Hinton PLAST computer code [24].

It must be mentioned that many other researchers used Owen & Hinton's code, in order to develop new software for the non-linear analysis of masonry. The most representative of these, is a non-linear analysis computer code developed by Adreaus [1]. The main disadvantages of the Owen & Hinton software, is the isotropic consideration of the materials and the use of isotropic yield criteria.

The software used in the present work, overcome the above-mentioned disadvantages of PLAST, and is appropriate to model the anisotropic behaviour of masonry, allowing the use of the regular yield surfaces developed (Eqs. 13 and 14). This specific iterative plane stress finite element program is based on four-noded isoparametric quadrilateral elements and is used to simulate the incremental loading and progressive failure of masonry under in-plane loads. The effectiveness of the program is demonstrated by comparing the computed behaviour with the analytical results of Adreaus [1].

During the development phase, special attention has been given in producing a visual representation of the analysis procedure and of the response results (Figure 7). In particular, the user is able to follow the individual stages of the analysis, as-it-progresses (i.e., for each load increment), by observing:

- a) the flow-chart diagram produced on the screen; which gives information on the individual operation performed within the program, the number of iterations needed for convergence within each load increment, and the computer run time required,
- b) the load-displacement diagram, and
- c) the coloured graphic images of the yield process, produced for each individual element within the structure, according to the kind of stress under which yield takes place (i.e., yield under biaxial compression, tension or heterosemous stress).

This visual representation of the analysis procedure is particularly useful to the user, not only for the instant information it provides as the software runs, but also for the verification of the results produced.

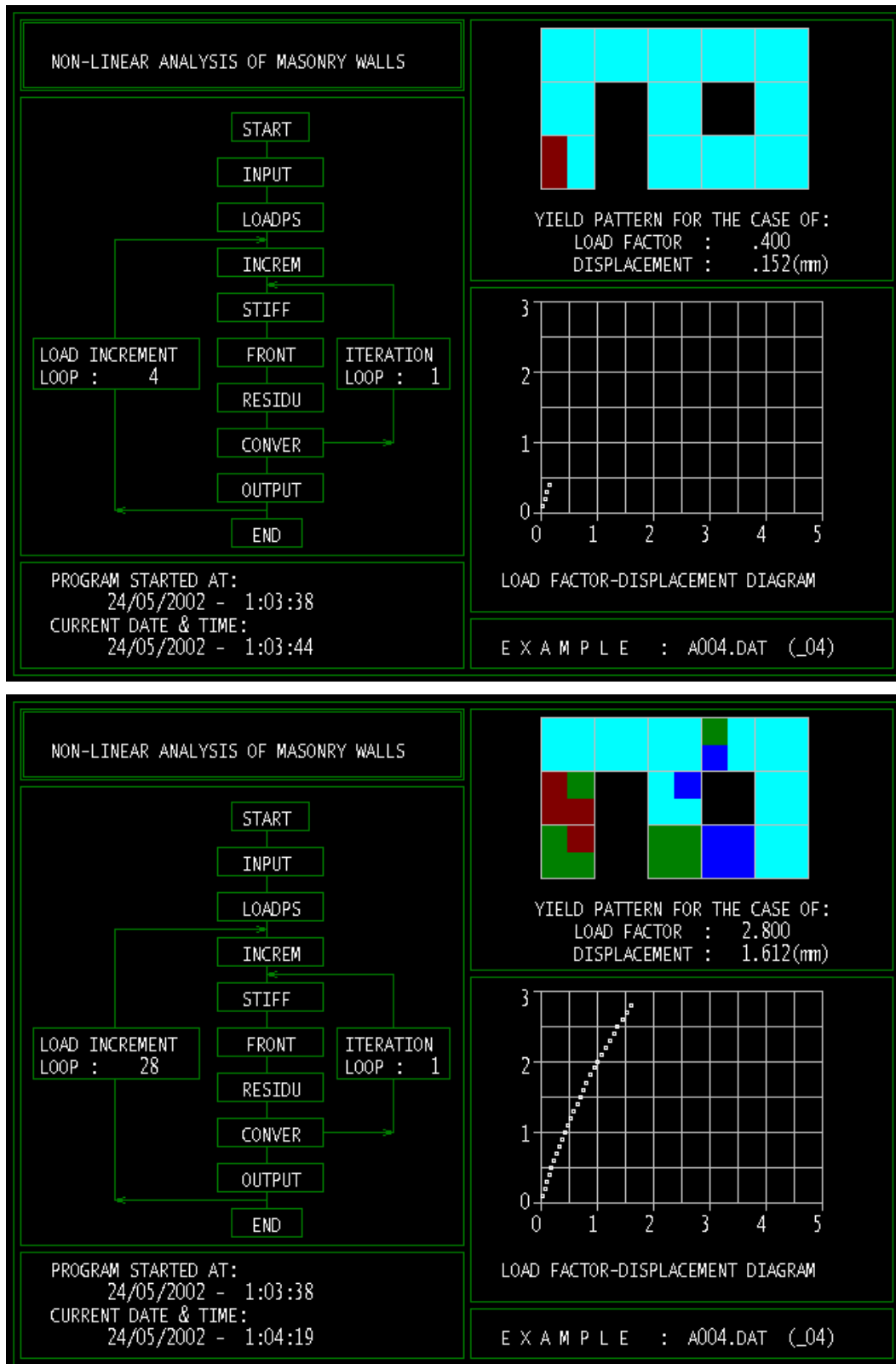


**Figure 7:** Load-displacement diagram and coloured image of the yield pattern within the structure, for every increment of load.

## 6 Numerical example

Using the computer program developed, we studied the non-linear behaviour of a URM shear wall with openings ([Figure 8](#)) under uniform compressive and shear loading, and with the following assumptions:

- The wall is perfectly fixed at the ground level and is acted upon by both horizontal and vertical loads, which are proportionally increased up to failure, according to the load factor  $\lambda$ . The loads are uniformly distributed at the wall top; the reference load amplitude in both directions is assumed to equal  $0.1 \text{ N/mm}^2$  and the load factor increment, equal to 0.1.
- The masonry wall has been discretized by means of four-node isoparametric quadrilateral elements, whose length is 1.00 m.
- Both isotropic and anisotropic behaviour has been assumed for the masonry material, with Young's modulus  $E=5700 \text{ N/mm}^2$  and Poisson's ratio  $\nu=0.19$ , for the isotropic case study, and moduli of elasticity  $E_x=4500 \text{ N/mm}^2$  and  $E_y=7500 \text{ N/mm}^2$  and Poisson's ratios  $\nu_{xy}=0.19$  and  $\nu_{yx}=0.32$  respectively, for the anisotropic case study.
- Both the simplified and the general yield criterion developed, have been used for the analysis.

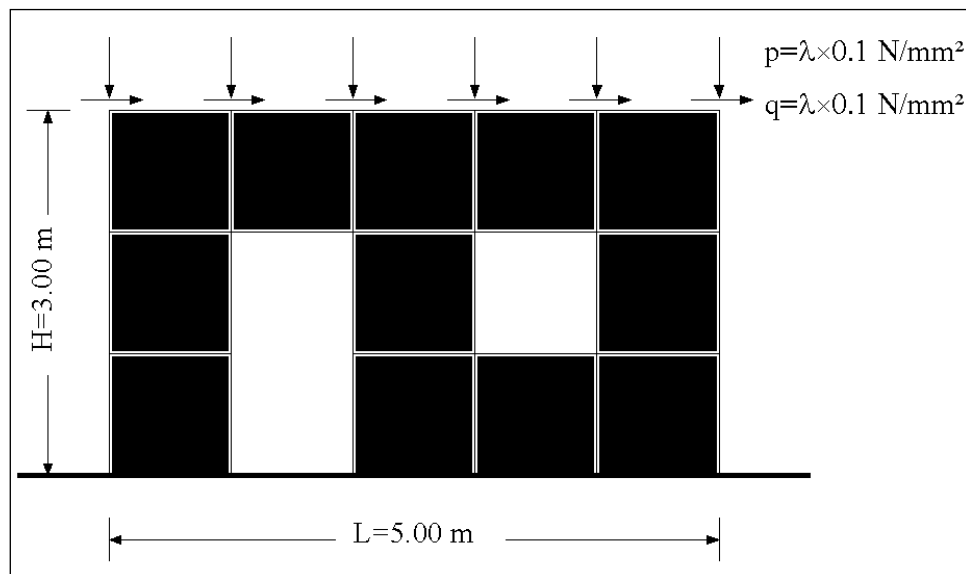


**Fig. 8** Unreinforced masonry shear wall with openings under both horizontal and vertical loads.

Using the method described, the diagram of the load factor  $\lambda$  versus displacements at the top of the masonry wall is computed and compared, in [Figure 9](#), with the corresponding analytical results taken from Andreaus [\[1\]](#). It is clearly shown that there is a good agreement between the results of the present non-linear analysis, using the simplified yield criterion of Eq. 23, and the results derived from Andreaus [\[1\]](#). This was expected, however, due to the fact that the same assumptions have been made for the analysis.

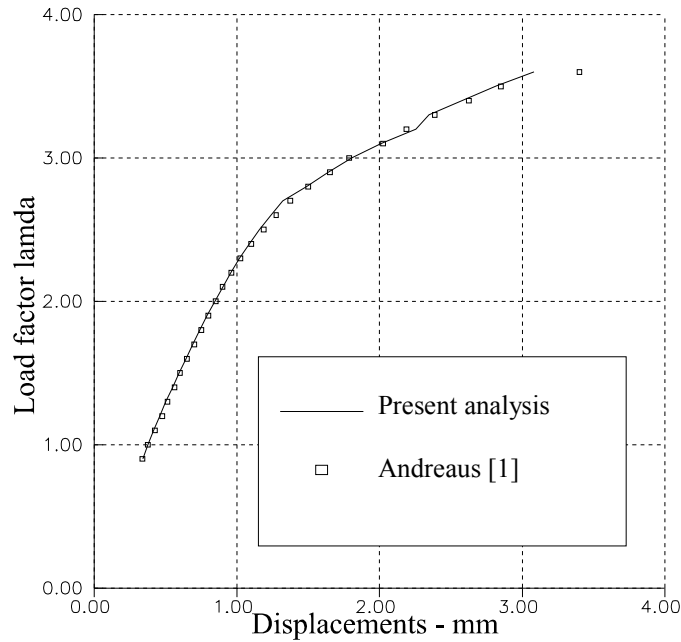


**Figure 9:** Load factor  $\lambda$  ( $\lambda$ )-displacement diagram.

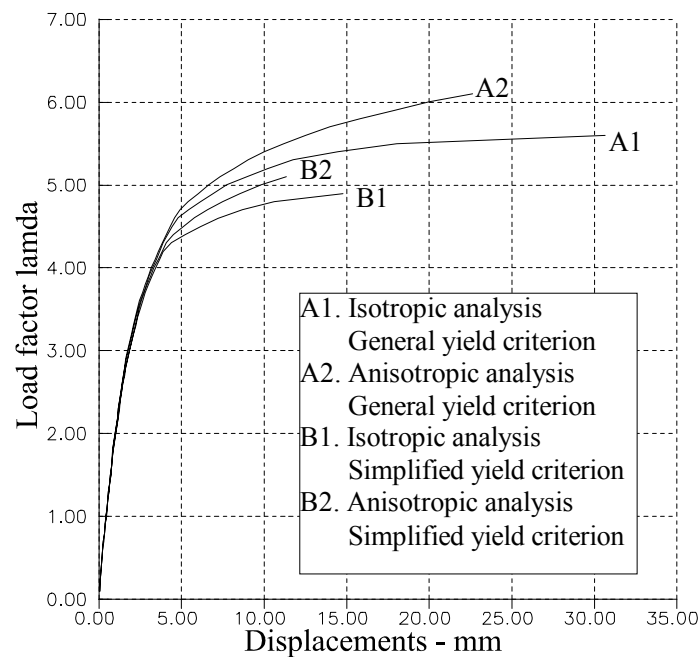


**Figure 10:** Load factor  $\lambda$  ( $\lambda$ )-displacement diagram.

[Figure 10](#) shows the diagram of the load factor  $\lambda$  versus displacement, using both the simplified and the general yield criterion proposed, and assuming the masonry material to be either isotropic or anisotropic. It is clear that non-linear behaviour of masonry is affected by the yield criterion used for the analysis. Although both criteria adopted have the same mechanical masonry characteristics (same mono-axial compressive and tensile strength as well as the same strength in pure shear), a strong variation of the load-displacement curves appears (curves A1 and B1).

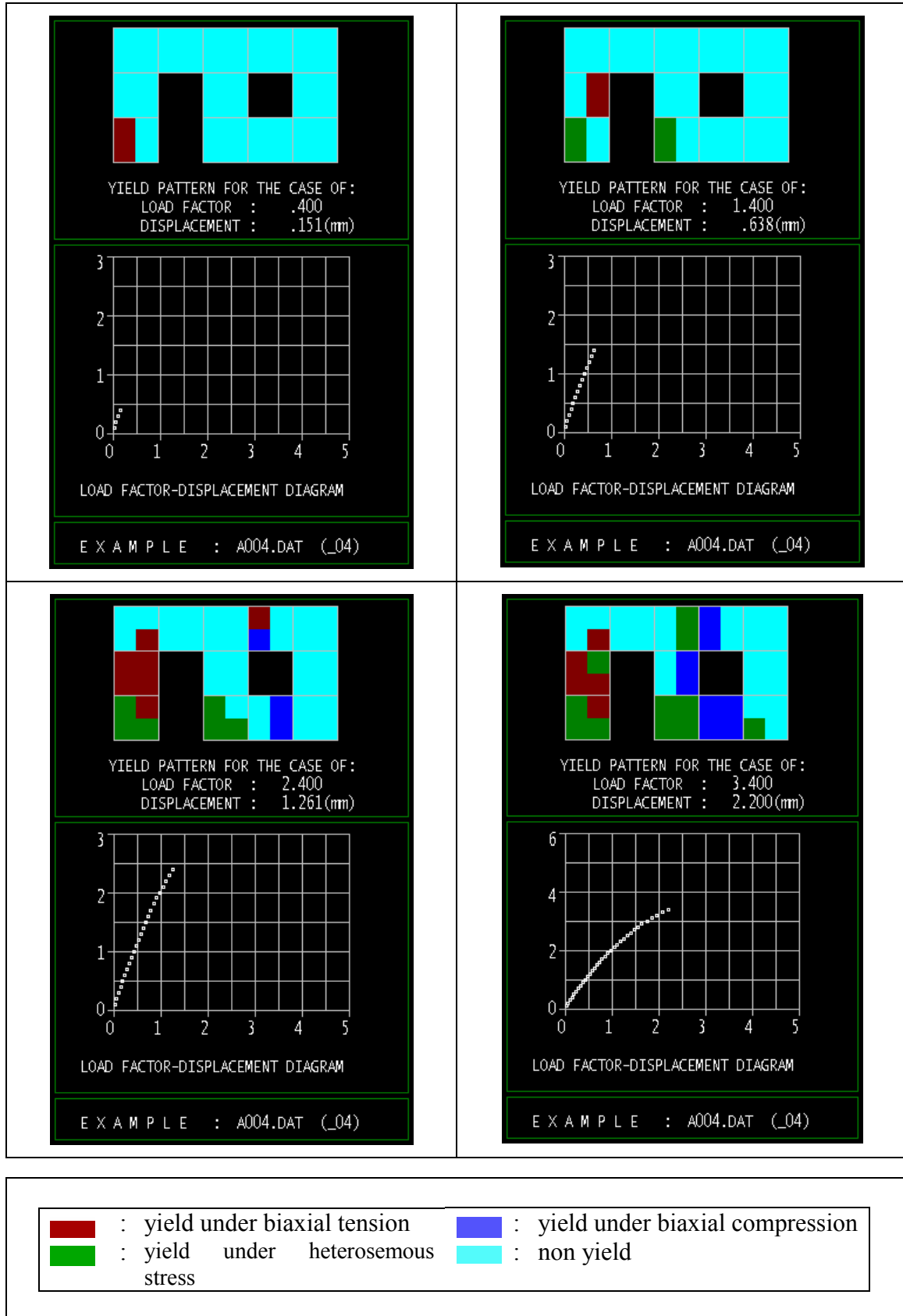


**Figure 11** Successive representations of yield pattern ( $\lambda=0.4, 1.4, 2.4, 3.4$ ).

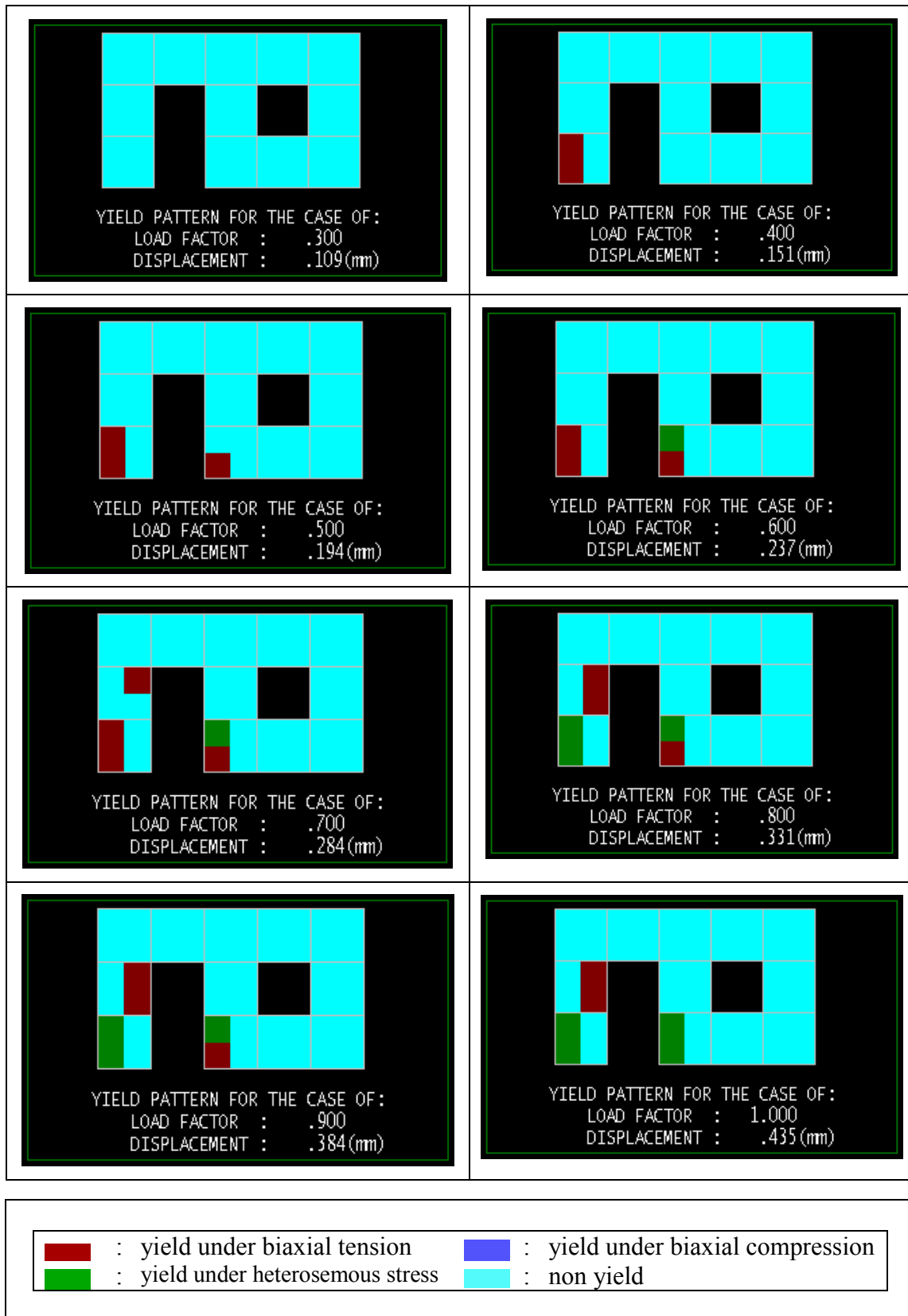


Figure 12: Successive representations of yield pattern ( $\lambda=0.3 - 1.0$ ).

It is also clear from [Figure 10](#), that non-linear behaviour of masonry is affected by the anisotropy of the masonry material. It must be noted that the consideration of the anisotropic behaviour of masonry leads to a greater ultimate load and to a less ultimate displacement (curves A2 and B2); thus, to a more brittle behaviour of masonry.

With the computer software developed, apart from the load-displacement diagram, graphic images of the yield process can be produced for every increment of load ([Figure 11](#)). These images are coloured according to the kind of stress under which yield takes place for every particular element (i.e., yield under biaxial compressive, tensile or heterosemous stress). These graphic images are especially useful not only because of the visual information they give, but also because of the validation they provide. As an example, in [Figure 12](#), and for a load factor of  $\lambda=0.7$ , the bottom left hand corner element yields first under biaxial tension; whereas, for a load factor of  $\lambda=0.8$ , the element yields under heterosemous stress.

## 7 Conclusions

The present work applies a new methodology for the non-linear 2D finite element analysis of anisotropic masonry under monotonic loading. The methodology focuses on the definition / specification of a general yield surface for the case of anisotropic masonry under biaxial stress state, as well as on the numerical solution of this non-linear problem. In particular, in order to define the yield surface a cubic tensor polynomial has been adopted, and the initial stress method has been applied for the solution of the elasto-plastic problem. The proposed failure surface is expressed in a unique mathematical form of all possible combinations of plane stress, to make it easier to include it into existing software for the analysis of masonry.

The main advantage of the method is that the formulation of the plasticity equations through a regular yield surface, leads to the elimination of the problem that occurs by the use of a singular surface. Results from the study of the non-linear behaviour of URM wall panels, under uniform compressive and shear loading, clearly state that the non-linear behaviour of masonry is strongly affected by the yield criterion used, as well as by the anisotropy of its material.

It is believed that the analytical method presented, describing the masonry failure surface in a simple manner, should be an effective tool for future investigations of the behaviour of masonry structures.

## REFERENCES

1. U. Andraeus, "Failure criteria for masonry panels under in-plane loading", J. Struct. Engrg., ASCE, **122**, (1), 37-46, 1996.
2. P.G. Asteris, "Analysis of anisotropic nonlinear masonry", PhD thesis, Dept. of Civ. Engrg., National Technical University of Athens, Greece, 2000.
3. A.W. Page, "Finite element model for masonry", J. Str. Div., ASCE, **104**, (8), 1267-85, 1978.
4. S.Ali, and A.W. Page, "Finite element model for masonry subjected to concentrated loads", J. Str. Div., ASCE, **114**, (8), 1761-84, 1988.
5. P.B. Lourenco, and J.S. Rots, "On the use of micro-modelling for the analysis of masonry shear-walls", Proceedings of the Second International Symposium on Computer Methods in Structural Masonry", Wales, U. K., 6-8 April 1993, pp. 14-26.
6. P.B. Lourenco, and J.S. Rots, "Understanding the behaviour of shear walls: A numerical review", Proceedings of the 10<sup>th</sup> International Brick/Block Masonry Conference, Alberta, Canada, 5-7 July 1994, pp. 11-20.
7. P.B. Lourenco, "Computational strategies for masonry structures", Dissertation, Dept. of Civ. Engrg., Delft University of Technology, 1996.
8. A.D. Tzamtzis, "Dynamic finite element analysis of complex discontinuous and jointed structural systems using interface elements", PhD Thesis, Department of Civil Engineering, QMWC, University of London, 1994.

9. D.J. Sutcliffe, H.S. Yu, and A.W. Page, "Lower bound limit analysis of unreinforced masonry shear walls", *Computer and Structures*, **79**, 1295-1312, 2001.
10. R. Hill, "The Mathematical Theory of Plasticity", Oxford University Press, 1960.
11. O.C. Zienkiewicz, S. Valliapant, and I.P. King, "Elasto-plastic solutions of engineering problems; 'initial stress' finite element approach", *Int. J. for Numerical Methods in Engrg.*, **1**, 75-100, 1969.
12. W.T. Koiter, "Stress-strain relations, uniqueness and variational theorems for elastic-plastic materials with a singular yield surface", *Quarterly of applied mathematics*, Vol. **XI**, 350-354, 1953.
13. U. Andraeus, and L. Ippolity, "A two-storey masonry wall under monotonic loading: a comparison between experimental and numerical results", *Proceedings of the 4<sup>th</sup> International conference on structural studies of historical buildings*, 319-326, Crete, Greece, 1995.
14. G. Ballio, M. Calvi, and G. Magenes, "Experimental and numerical investigation on a brick masonry building prototype", Reports 1.1, 2.0, 3.0, Consiglio Nazionale delle Ricerche, Gruppo Nazionale per la Difesa dai Terremoti, Italy, 1992.
15. D.C. Drucker, "A more fundamental approach to plastic stress-strain solutions", *Proceedings of the 1<sup>st</sup> U. S. natn. Cong. Appl. Mech.*, 487-491, 1951.
16. W. Prager, "A new method of analyzing stress and strain in work hardening plastic solids", *Revue Méc. Appl., Buc.*, **23**, 493-496, 1956.
17. S.W. Tsai, and E.M. Wu, "A general failure criterion for anisotropic materials", *Journal of Composite Materials*, Vol. 5, 58-80, 1971.
18. E.M. Wu, "Optimal experimental measurements of anisotropic failure tensors", *Journal of Composite Materials*, Vol. 6, 472-480, 1972.
19. Z. Jiang, and R.C. Tennyson, "Closure of the cubic tensor polynomial failure surface", *Journal of Composite Materials*, Vol. 23, 208-231, 1989.
20. E.M. Wu, and J.K. Scheublein, "Laminate Strength - A Direct Characterization Procedure", *Composite materials: Testing and Design (Third Conference)*, ASTM STP 546, American Society for Testing and Materials, 188-201, 1974.
21. C.A. Symakezis, and P.G. Asteris, "Masonry failure criterion under biaxial stress state", *ASCE J. Mat. in Civ. Engrg.*, **13**(1), 58-64, 2001.
22. M. Dhanasekar, A.W. Page, and P.W. Kleeman, "The failure of brick masonry under biaxial stresses", *Proc. Instn Civ. Engrns, London, England*, **79**, (2), 295-313, 1985.
23. A.W. Page, "The biaxial compressive strength of brick masonry", *Proc. Instn Civ. Engrs*, **71**, (2), 893-906, 1981.
24. D.R.J. Owen, and E. Hinton, "Finite Elements in Plasticity: Theory and Practice", Pineridge Press Ltd., Swansea, U.K., 1982.

## APPENDIX

The following notations have been used in this paper:

### *Symbols*

- $D$  = Elasticity matrix;  
 $D_{ep}$  = Elasto-plastic matrix;  
 $E$  = Young's modulus for isotropic assumption of the material behaviour;  
 $E_x, E_y$  = module of elasticity in the x and y-direction respectively;  
 $F_i$  = strength tensor second rank;  
 $F_{ij}$  = strength tensor fourth rank;  
 $F_{ijk}$  = strength tensor sixth rank;  
 $G_{xy}$  = shear modulus in the x, y-plane;  
 $\alpha$  = flow vector;  
 $\theta$  = angle between maximum principal stress direction and direction of x-axis;  
 $\lambda$  = plastic multiplier as well as load factor;  
 $\nu$  = Poisson's ratio for isotropic assumption of the material behaviour;  
 $\nu_{xy}, \nu_{yx}$  = Poisson's ratios in the x, y and y, x-plane respectively;  
 $\sigma_x, \sigma_y$  = normal plane stress along x-axis and y-axis respectively;  
 $\sigma_1, \sigma_2$  = maximum and minimum principal stresses, respectively; and  
 $\tau$  = shear stress measured in the x, y-plane.

### *Indexes*

- $e$  = elastic;  
 $p$  = plastic; and  
 $ep$  = Elastoplastic.

### *Colours*

-  = yield under biaxial tension;  
 = yield under heterosemous stress;  
 = yield under biaxial compression; and  
 = non yield.